Canadian Conference - Pacific Conference on Earthquake Engineering 2023

Vancouver, British Columbia

June 25th – June 30th, 2023

Fracture Resistance of Moment Frame Beam-Column Connections with Cope Holes under Seismic Loading

Mehdi Bashiri[1*], Gregory MacRae[2] and Liang-Jiu Jia[3]

[1]PhD Student, Department of Civil and Natural Resources Engineering, University of Canterbury, Christchurch, New Zealand
[2]Professor, Department of Civil and Natural Resources Engineering, University of Canterbury, Christchurch, New Zealand
[3]Associate Professor, Department of Disaster Mitigation for Structures, College of Civil Engineering, Tongji University, Shanghai, China
[*]mehdi.bashiri@pg.canterbury.ac.nz (Corresponding Author)

ABSTRACT

Welded steel connections are widely used in structures located in high seismic hazard zones. To discourage fracture under repeated loading and inelastic member deformation, the weld sizes are generally selected based on the maximum force demand, while the weld details (materials and processes) are covered by specific requirements to ensure ductility. Even given that some minimum requirements exist, some connection types may suffer Ultra-Low Cycle Fatigue (ULCF) fracture before others, when subjected to earthquake shaking. While a number of UCLF models are available, most are either too complex or insufficiently precise. This research presents ULCF fracture analysis of beam-column welded connections with cope holes using ABAQUS software. Initially, a fracture model that is both precise and straightforward is presented and validated through four small coupon specimens and a large-welded connection. Relationships between a strain-based demand amplitude, *A*, and the number of cycles to that demand amplitude, *N* (i.e. *A*-*N* relationships), are then developed with the fracture model which includes kinematic and isotropic hardening. It is shown that the fracture model is accurate enough to predict the ductile fracture behaviour of steel. Additionally, the A-N curves are considered to be practical tools for assessing the remaining earthquake life of structural steel due to their low scatter and accuracy.

Keywords: Ductile fracture, Ultra-low cycle fatigue, Strain-based-N curve, Finite element analysis, Cope hole.

INTRODUCTION

Earthquakes have always been a threat to human life led to casualties and damage. Many of these problems result from failure or irreparability. In many structural types (steel, timber, and concrete), it is the steel elements that are designed to be the weakest and to dissipate the energy. Fracture in steel during an earthquake generally occurs under only a few cycles of loading which is defined as Ultra-Low Cycle Fatigue (ULCF) fracture. The fracture surface is similar to that from monotonic experiments, and it may be different from that of High-Cycle Fatigue (HCF).

Failure of steel is generally by fracture, and structures may be irreparable if they are close to fracture, even if the fracture has not occurred. In order to design structures to behave well under one or more earthquake events, it is desirable to know how many cycles they can sustain before fracture. Also, to assess the remaining life of a structure that has been damaged during an earthquake, fracture considerations are important.

Strong shakings can cause structural elements to yield. As a result, when determining the relationship between the demand amplitude, *A*, and the number of cycles to that amplitude, *N*, defined as the *A*-*N* relationship, it is not appropriate to use *A* based on stress as in the case of HCF where stress-N curves are used. Instead, a strain-based *A*-*N* relationship is more likely to predict the fracture behaviour of steel members.

It may be seen from the discussion above that for engineers to design structures of any material, in which steel elements are yielding and dissipating energy, there is a need for them to develop strain-based *A*-*N* curves as one of the decision-making tools for the remaining earthquake life of the steel structures. This paper seeks to address this need by developing methods to model the initiation of fracture in pure steel using an ultra-low cycle fatigue approach. In particular, answers are sought to the following questions:

1. Can a model be developed and applied to structural steel?
2. How does it describe the behaviour of a large-scale welded connection?
3. Can a strain-based *A-N* curve be developed for a welded connection?

LITERATURE

Numerous studies have focused on evaluating the ductile fracture of structural steel, and a variety of methods have been proposed to predict this type of fracture. These methods include the void growth method (VGM), Continuum damage mechanics (CDM), and stress modified critical strain (SMCS) [1-4]. According to the VGM fracture mechanism, voids grow within a ductile material as the loading increases. The VGM predicts the void growth process by considering the combination of stress triaxiality, *T*, and equivalent plastic strain ε_{eq}^{pl} which can be expressed as shown in Eq. (1).

$$ln\left(\frac{R}{R_0}\right) = 0.283\int_0^{\varepsilon_{eq}^{pl}} e^{\frac{2}{3}T}\, d\varepsilon_{eq}^{pl} \tag{1}$$

where R_0 and *R* are the initial and current radius of the void, respectively. The VGM assumes that ductile fracture occurs when the ratio R/R_0 reaches a threshold value.

The SMCS approach also considers the void growth with the assumption that cracks initiate at a critical plastic strain. Kanvinde et al. conducted finite element (FE) analyses on twelve pull-plates to assess the effectiveness of both VGM and SMCS in predicting ductile fracture. The findings indicated that these methods are more precise than basic longitudinal strain criteria [5]. In another study, Liao et al. utilized VGM and SMCS to examine the ductile fracture of welded connections. The VGM presented a superior performance to the SMCS method under monotonic loading, although calibration via scanning electron micrograph was still required [6].

The problem of balancing accuracy and simplicity in ductile fracture analysis has always been a challenge. To address this issue, Jia proposed a new approach for analyzing ULCF fracture in structural steel, which is based on the VGM [7-9].. The method is straightforward and can be calibrated using only the tensile coupon test of the steel. Jia's approach uses Miner's rule to incorporate a failure threshold into the VGM. By considering the loading history, Miner's rule calculates the cumulative damage index, *D*. The point at which *D* reaches 1 signifies the occurrence of void coalescence and crack formation. Experiments have revealed that no significant damage occurs when *T* is below -1/3. Jia's proposed equations, Eq. (2) and Eq. (3) present the fracture strain, ε_f and *D* proposed by Jia.

$$\varepsilon_f = x_{cr}.\, e^{-1.5T} \tag{2}$$

$$dD = \begin{cases} \dfrac{d\varepsilon_{eq}^{pl}}{x.\, e^{-1.5T}} & T > -\dfrac{1}{3} \\ 0 & T \leq -\dfrac{1}{3} \end{cases} \tag{3}$$

where x_{cr}, is a model parameter obtained by trial-and-error.

To perform a ductile fracture analysis and accurately simulate the post-yield behavior of a material, a plasticity model is necessary. The Chaboche plasticity model with isotropic hardening is a suitable option for modeling the post-yield behavior of steel due to its accuracy and simplicity [10]. For ductile fracture analysis, the Chaboche model with true stress and true strain data is preferred because the stress state is no longer uniaxial after necking [11]. The true stress and true the strain data can be obtained from engineering stress and engineering strain using Eq. (4) and Eq. (5), respectively [12].

$$\sigma_t = \sigma_e(1 + \varepsilon_e) \tag{4}$$

$$\varepsilon_t = ln\,(1+\varepsilon_e) \tag{5}$$

Where σ_t and ε_t are true stress and true strain, respectively. Also, σ_e and ε_t are engineering stress and engineering strain that are obtained from the tensile coupon test.

Jia et al. introduced a technique for calibrating the post-necking behavior of steel in order to accurately predict its material properties. The method, known as the modified weighted average method (MWA), incorporates a linear model for the post-necking portion of the stress-strain curve, as illustrated by Eq. (6) [7].

$$\sigma = \sigma_{neck} + w.\sigma_{neck}(\varepsilon - \varepsilon_{neck}) \tag{6}$$

where σ_{neck} and ε_{neck} are stress and strain at the point of necking. The factor w is then determined through a trial-and-error process, which serves to calibrate the stress values for the post-necking region.

Xiang et el. showed the damage that occurs in steel during a cyclic loading is related to the hardening type i.e., isotropic hardening (IH) and kinematic hardening (KH) [13]. It was shown that the damage related to KH is less than that of IH. Therefore, Eq. (7) was proposed to adjust the damage for all loading regimes.

$$D_{ULCF} = D_{IH} + \eta.D_{KH} \tag{7}$$

Where D_{ULCF}, D_{IH}, and D_{KH} are ductile fracture damage, IH-related damage, and KH-related damage, respectively. Also, the factor, η, is applied to reduce KH-related damage which is suggested to be 0.3 for steel and aluminum. This improved approach was subsequently applied to analyze the progression of damage in a high-rise steel frame, and the accuracy of the model was confirmed through a comparison of the results obtained from both testing and finite element (FE) analysis [14, 15].

METHODOLOGY

Finite element analysis of coupon specimens

The study uses ABAQUS [16] software to conduct fracture analysis on structural steel to assess its performance when subjected to ULCF loading. The initial analysis involved examining small coupon specimens to validate and calibrate the model. Finite element (FE) analyses were performed on a round steel coupon which had been tested under both monotonic and cyclic loadings. Figure 1 shows the dimensions and the material properties of the round steel coupon. The Chaboche plasticity model and Jia's fracture approach were used to define the post-yield and ductile fracture behavior of the steel. Table 1 describes the mechanical properties of the steel. The middle section of the specimen had a substantial impact on its overall performance. Consequently, only this section was modelled to minimize the analysis time as shown in Figure 2.

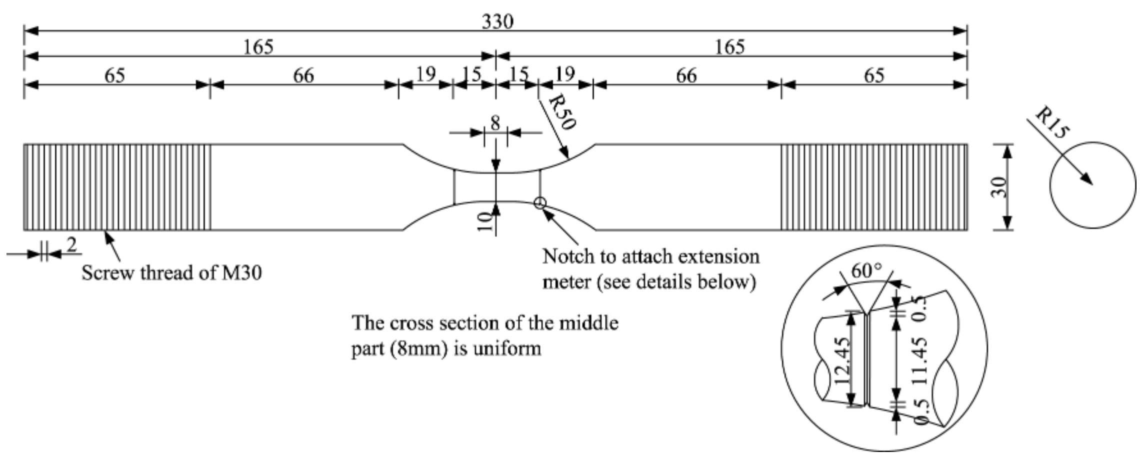

Figure 1 Characteristics of the tested specimen (units in mm) [8]

Table 1 Material propertises of the steel coupon specimen.

f_y(MPa)	c_1(MPa)	c_2(MPa)	c_3(MPa)	γ_1	γ_2	γ_3	Q_∞	b	X_{cr}
255	2484.9	107.05	107.05	19.22	0	0	156.62	18.11	2.15

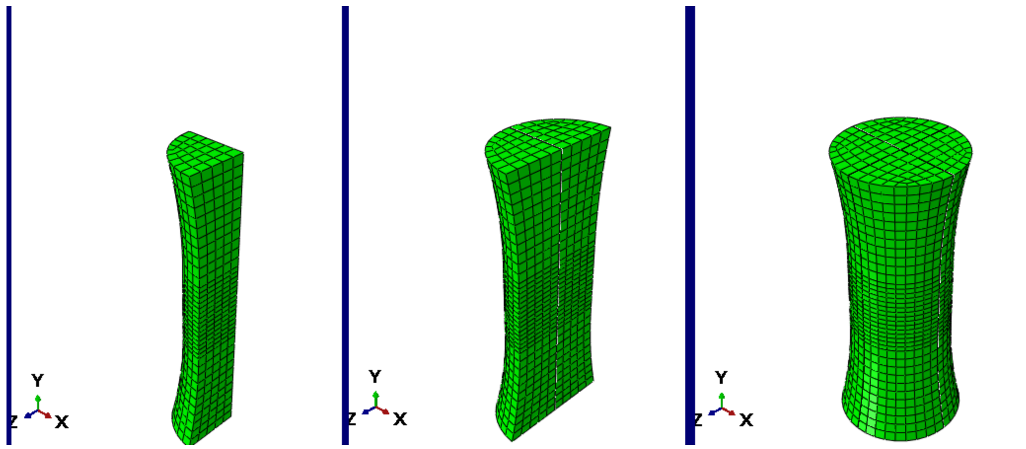

Figure 2 FE model of the steel coupon specimen

The loading protocol used in the experiment is presented in Figure 3. Initially, the FE model was calibrated using monotonic loading, and subsequently, it was verified through cyclic loadings.

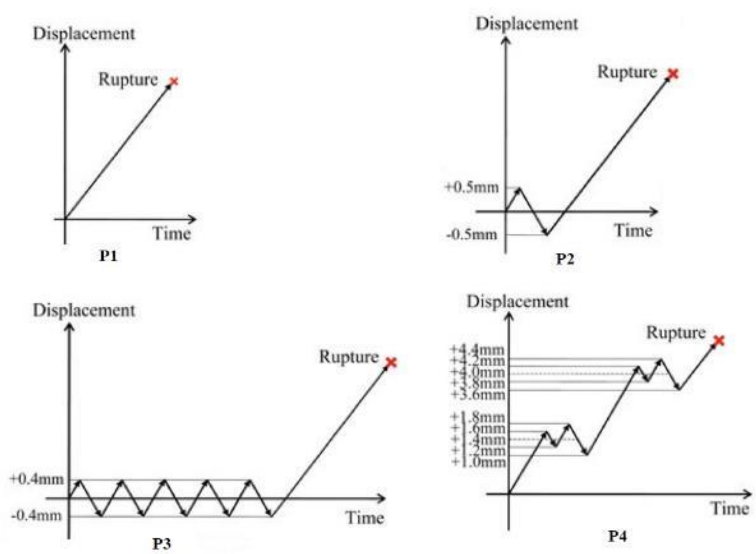

Figure 3 Loading protocols of the tested specimens.

Finite element analysis of a large-scale welded connection

The effectiveness of the proposed method for analyzing large-scale structural elements was evaluated through investigation of the ULCF fracture in a welded beam-to-column connection which was tested under constant amplitude loading. The connection details are presented in Figure 4. SM490 steel with a yield stress of 339 MPa was used for the connection. The loading protocol used for the connection is shown in Figure 5.

Figure 6 shows the welded connection FE model. The connection was modelled using C3D8R elements. Finer mesh sizes were considered for areas with high stress concentration compared to the rest of the connection. The elastic behavior was assigned to the end part of the beam flanges to simulate the butt welds. Also, three mesh arrangements were used to make sure the results are mesh independent. The model was first calibrated using test results, after which it was employed to develop *A-N* curves.

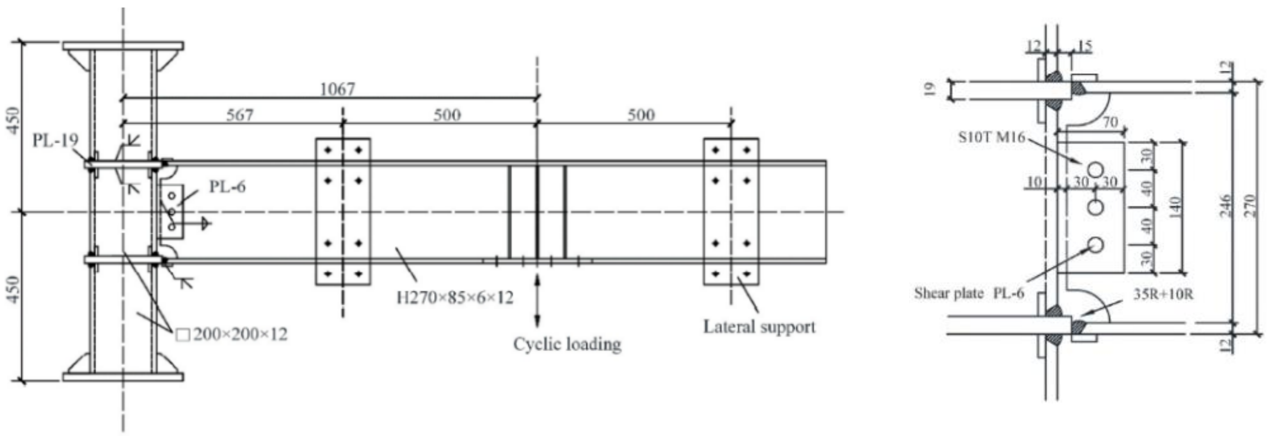

a) Global view

b) Connection details

Figure 4 Characteristics of the tested beam-to-column connection (units in mm) [15]

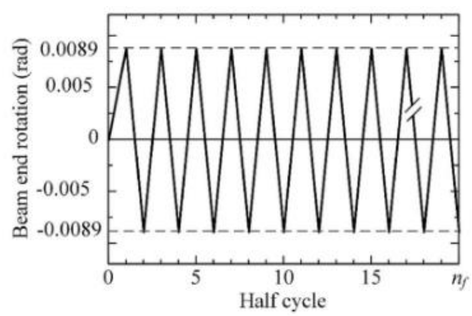

Figure 5 Loading protocol of tested connection.

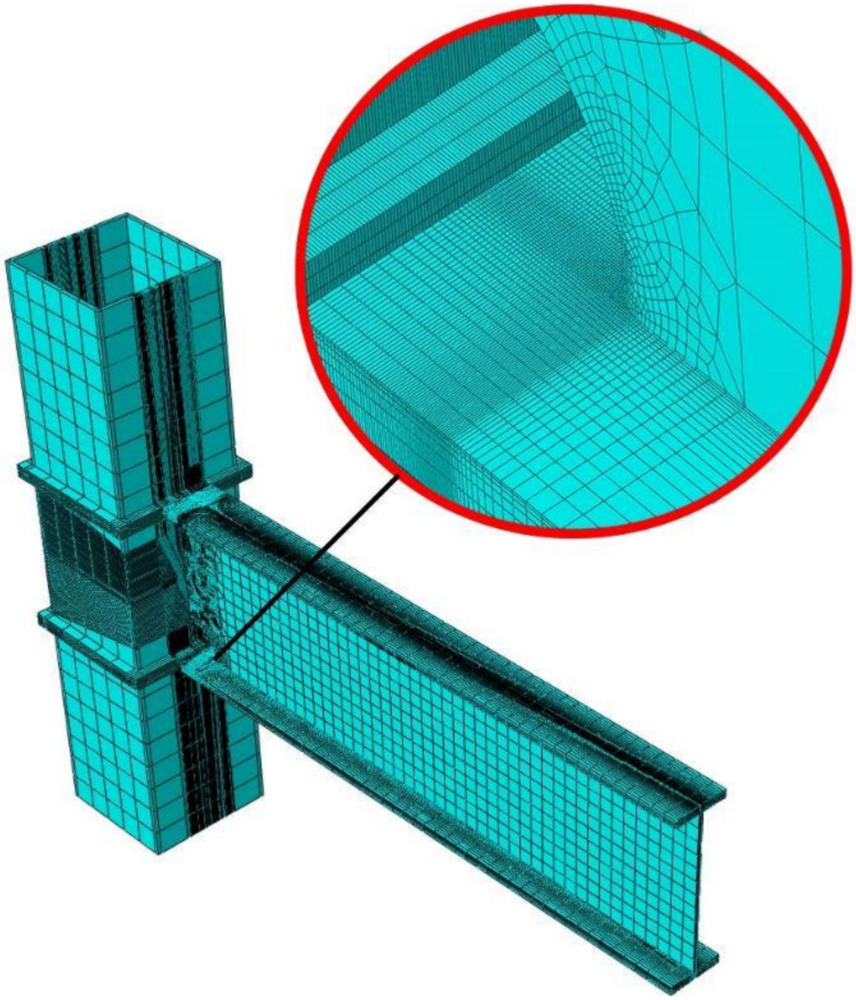

Figure 6 FE model of the welded connection

Development of strain-based *A-N* curve

A-N curves were developed for the connections in order to develop a tool to estimate the earthquake life of the connection. Strain-N curves were first considered as the *A-N* curve. However, the determination of strain is dependent on the precise definition of the plastic hinge length, L_p, which is not well-defined. To resolve this issue, plastic rotation, θ_p, was employed as a substitute for strain. The plastic rotation, which is obtained from $(\delta\text{-}\delta_y)/L$ where δ, δ_y, and L are total displacement, elastic displacement, and beam length, respectively, is a convenient indicator of plastic damage due to its direct correlation with plastic strain, as well as its ease of measurement and computation. Therefore, θ_p-*N* curves were considered as the A-N curve. Four constant-amplitude cyclic loadings with different rotation angles were applied to the free end of the beam. The maximum plastic rotation and the number of cycles before crack initiation were recorded to develop A-N curves.

RESULTS AND DISCUSSIONS

Figure 7 indicates force-displacement diagrams of the coupon specimen subjected to various loading regimes. The results show the numerical model predicted both the monotonic and cyclic behaviour very well.

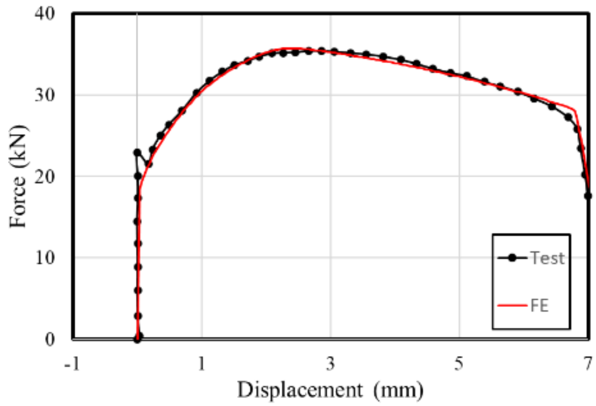

a) Load regime P1

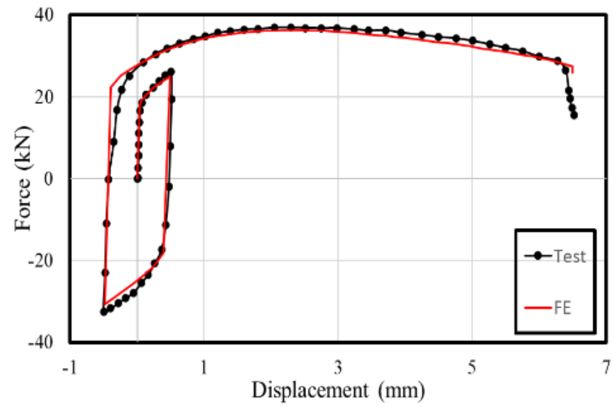

b) Load regime P2

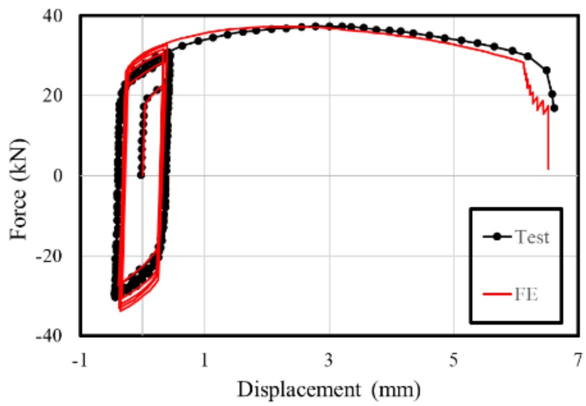

c) Test regime P3

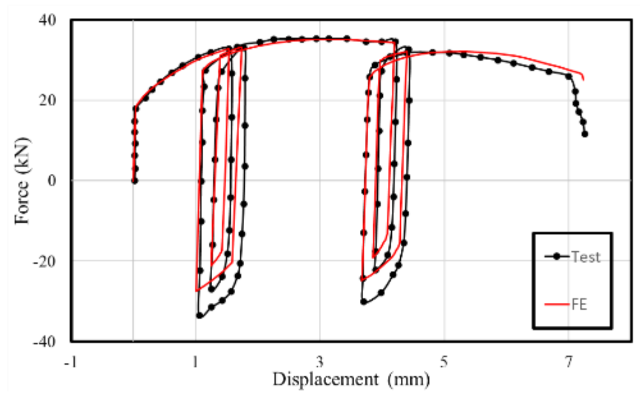

d) Load regime P4

Figure 7 Comparison between FE and test force-displacement diagram for coupon specimens

The welded connection started to fracture after 15 cycles in the test. So, x_{cr}=0.75 was selected in a way that the FE model fracture initiation occurs after 15 cycles. Figure 8(a) and (b) show the damage index of the FE model and fracture pattern obtained from the test, respectively. It can be observed that fracture initiated at the edge of the cope hole and the model predicated the fracture pattern very well.

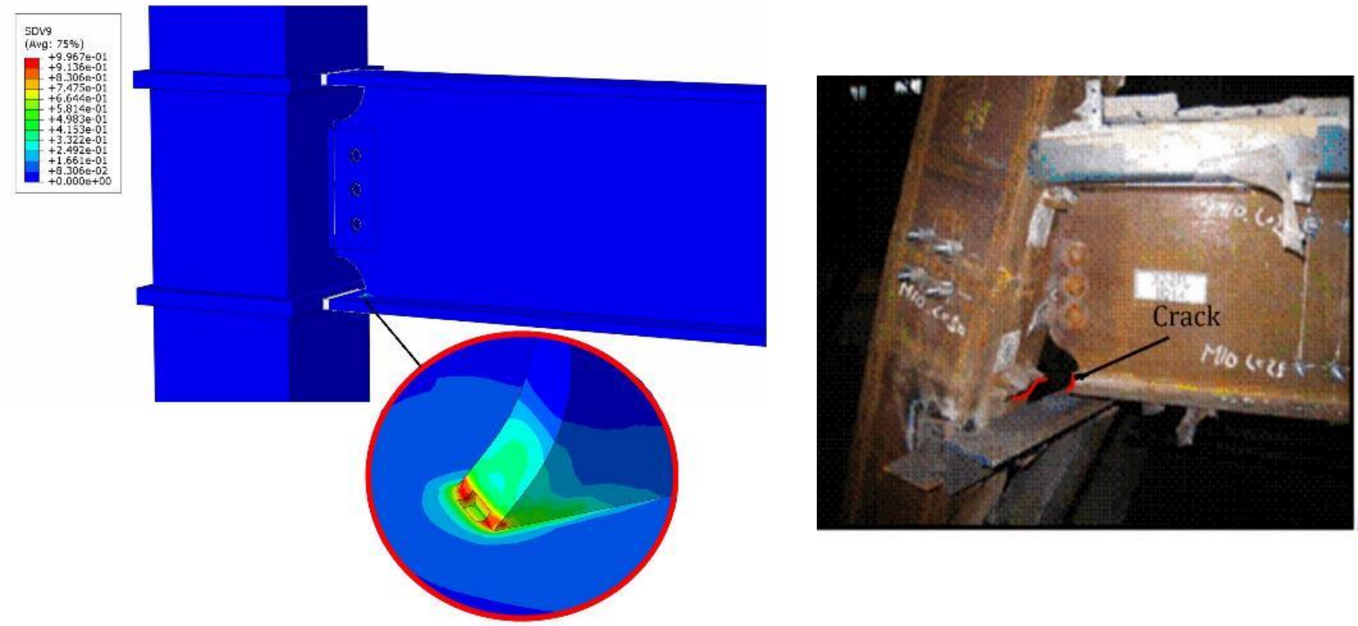

b) Crack location of the welded connection

a) Damage index of FE model

Figure 8 Comparison between FE model and test crack pattern

Figure 9 shows the connection θ_p-N curve in a logarithmic scale. It can be seen that empirical equations of the form $\theta_p = 0.032N^{-1.184}$ represent the ductile fracture behaviour of the connection with a very low scatter, R^2=0.974.

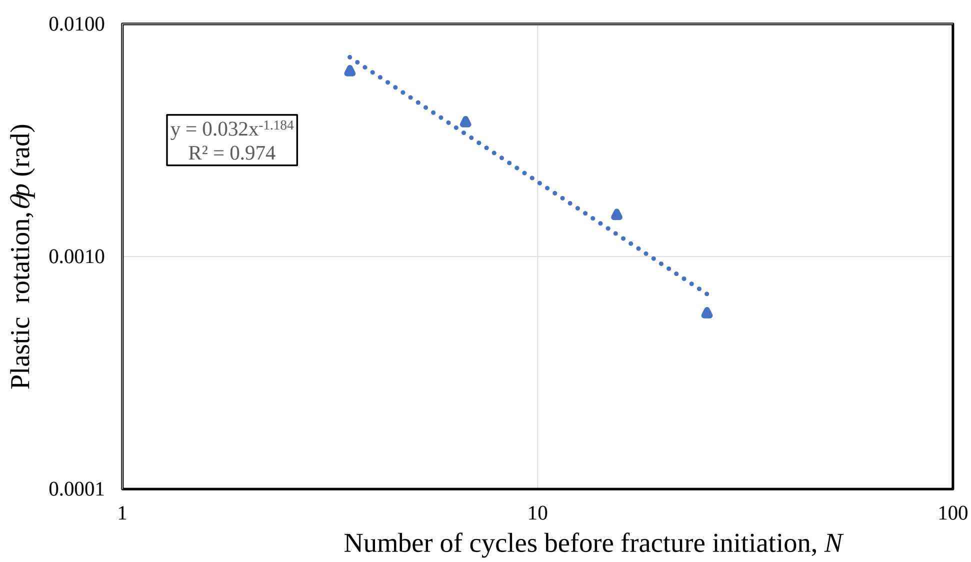

Figure 9 θ_p-N curve of the welded connection

Figure 10 indicates the comparison between *A*-*N* curves for models with three different mesh arrangements, where the minimum mesh size varies from 0.25mm to 1mm. The comparison shows that the m1 model with 1mm is slightly different from m2 with 0.5mm and m3 with 0.25mm minimum element size. However, m2 and m3 showed almost the same fracture behaviour that indicates that mesh arrangements with minimum mesh size equal or smaller than 0.5mm are mesh independent.

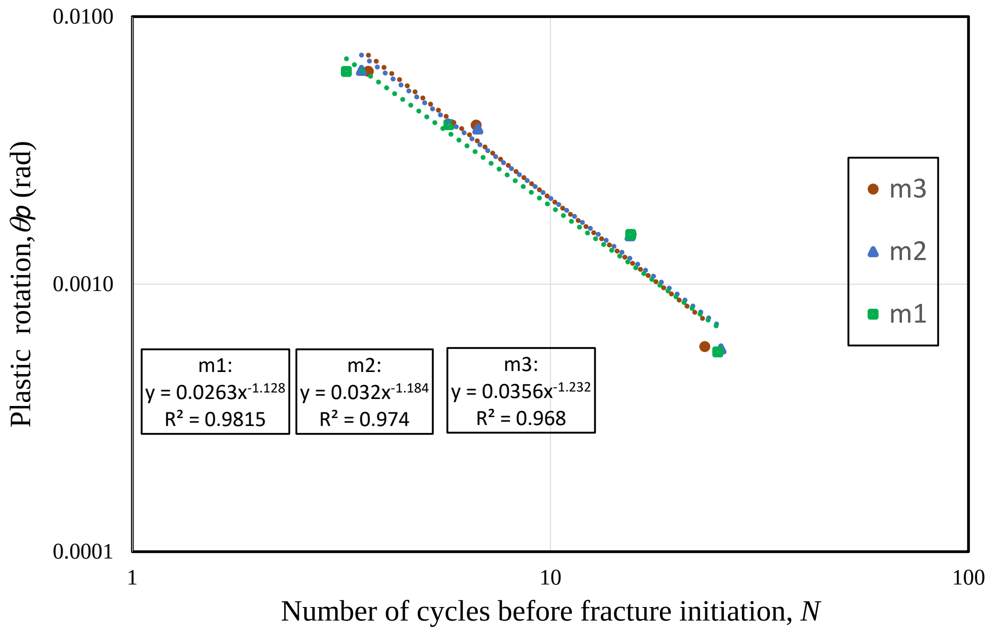

Figure 10 Mesh sensitivity of the FE model

1. CONCLUSIONS

This study presents ductile fracture analysis of structural steel in order to develop strain-based *A-N* curves to assess the remaining earthquake life of structural steel. Jia's fracture model was first verified with small scale coupon specimen as well as large-scale welded connection. The model was then employed to develop θ_p-*N* curve for the welded connection. The results determined from this study are:

a) The ULCF fracture method, in combination with the Chaboche plasticity model, offers a precise and straightforward approach for ductile fracture assessment in steel subjected to both monotonic and cyclic loads. The model's calibration is straightforward, and it shows minimal variation for comparable specimens.

b) For the large-scale welded connection, this approach predicts crack initiation time and location with accuracy. However, there is no crack propagation criteria yet for this model and needs to be considered in the future.

c) Low scatter strain-based *A-N* curves with empirical equations of the form $\theta_p = \alpha N^{-\beta}$,where α and β are fit parameters, can be obtained from ductile fracture analysis. These curves are practical tools for engineers to assess the remaining earthquake life of structural members.

ACKNOWLEDGMENTS

The authors are grateful to the Resilience to Natures Challenges program, under which this project is being conducted.

REFERENCES

[1] J. Hancock and A. Mackenzie, "On the mechanisms of ductile failure in high-strength steels subjected to multi-axial stress-states," *Journal of the Mechanics and Physics of Solids*, vol. 24, no. 2-3, pp. 147-160, 1976.

[2] L. M. KACHANOV, "Time of the rupture process under creep conditions, Izy Akad," *Nank SSR Otd Tech Nauk*, vol. 8, pp. 26-31, 1958.

[3] J. R. Rice and D. M. Tracey, "On the ductile enlargement of voids in triaxial stress fields∗," *Journal of the Mechanics and Physics of Solids*, vol. 17, no. 3, pp. 201-217, 1969.

[4] A. Mackenzie, J. Hancock, and D. Brown, "On the influence of state of stress on ductile failure initiation in high strength steels," *Engineering fracture mechanics*, vol. 9, no. 1, pp. 167-188, 1977.

[5] A. Kanvinde and G. Deierlein, "Finite-element simulation of ductile fracture in reduced section pull-plates using micromechanics-based fracture models," *Journal of Structural Engineering,* vol. 133, no. 5, pp. 656-664, 2007.

[6] F. Liao, W. Wang, and Y. Chen, "Ductile fracture prediction for welded steel connections under monotonic loading based on micromechanical fracture criteria," *Engineering Structures,* vol. 94, pp. 16-28, 2015.

[7] L.-J. Jia and H. Kuwamura, "Ductile fracture simulation of structural steels under monotonic tension," *Journal of Structural Engineering,* vol. 140, no. 5, p. 04013115, 2014.

[8] L.-J. Jia and H. Kuwamura, "Ductile fracture model for structural steel under cyclic large strain loading," *Journal of Constructional Steel Research,* vol. 106, pp. 110-121, 2015.

[9] L.-J. Jia and H. Ge, *Ultra-low-Cycle Fatigue Failure of Metal Structures Under Strong Earthquakes*. Springer, 2019.

[10] J. Chaboche, K. D. Van, and G. Cordier, "Modelization of the strain memory effect on the cyclic hardening of 316 stainless steel," 1979.

[11] L.-J. Jia and H. Kuwamura, "Prediction of cyclic behaviors of mild steel at large plastic strain using coupon test results," *Journal of Structural Engineering,* vol. 140, no. 2, p. 04013056, 2014.

[12] S. Tu, X. Ren, J. He, and Z. Zhang, "Stress–strain curves of metallic materials and post-necking strain hardening characterization: A review," *Fatigue & Fracture of Engineering Materials & Structures,* vol. 43, no. 1, pp. 3-19, 2020.

[13] P. Xiang, L.-J. Jia, M. Shi, and M. Wu, "Ultra-low cycle fatigue life of aluminum alloy and its prediction using monotonic tension test results," *Engineering Fracture Mechanics,* vol. 186, pp. 449-465, 2017.

[14] P. Xiang, Z. Qing, L.-J. Jia, M. Wu, and J. Xie, "Damage evaluation and ultra-low-cycle fatigue analysis of high-rise steel frame with mesoscopic fracture models," *Soil Dynamics and Earthquake Engineering,* vol. 139, p. 106283, 2020.

[15] M. Ministry of Education of Japan, "maintenance and recovery of functionality in urban infrastructures," 2013.

[16] K. Hibbit, "Sorensen, Inc.(2010) ABAQUS/Standard User's Manual, Version 6.10," *Pawtucket, RI, USA*.